

Doping and bond length contributions to Mn K-edge shift in $\text{La}_{1-x}\text{Sr}_x\text{MnO}_3$ ($x=0-0.7$) and their correlation with electrical transport properties

S. K. Pandey,^{1,*} R. Bindu,^{1,†} Ashwani Kumar,^{2,‡} S. Khalid,³ and A. V. Pimpale^{1,§}

¹*UGC-DAE Consortium for Scientific Research, University Campus, Khandwa Road, Indore 452 017, India*

²*School of Physics, Devi Ahilya University, Khandwa Road, Indore 452 017, India*

³*National Synchrotron Light Source, Brookhaven National Laboratory, Upton, NY - 11973, USA*

The room temperature experimental Mn K-edge x-ray absorption spectra of $\text{La}_{1-x}\text{Sr}_x\text{MnO}_3$, $x = 0 - 0.7$ are compared with the band structure calculations using spin polarized density functional theory. It is explicitly shown that the observed shift in the energy of Mn K-edge on substitution of divalent Sr on trivalent La sites corresponds to the shift in the center of gravity of the unoccupied Mn 4*p*-band contributing to the Mn K- absorption edge region. This correspondence is then used to separate the doping and size contributions to the edge shift due to variation in number of electrons in valence band and Mn-O bond lengths, respectively, when Sr is doped into LaMnO_3 . Such separation is helpful to find the localization behaviour of charge carriers and to understand the observed transport properties of these compounds.

PACS numbers: 61.10.Ht; 71.20.-b; 72.80.Ga

I. INTRODUCTION

In recent years, hole-doped manganese oxides have been the subject of intense research because of their various interesting properties: colossal magnetoresistance (CMR), charge ordering, orbital ordering, phase separation, *etc.*^{1,2,3}. The compounds under present study $\text{La}_{1-x}\text{Sr}_x\text{MnO}_3$, $x = 0 - 0.7$ also show these interesting properties for specific range of x ⁴. In this doping range the resistivity behaves in a non-monotonic fashion, first decreasing as x increases up to 0.4 and then increasing as x further increases for a wide temperature range, see figure 1c. This behaviour is not very well understood. Although double exchange mechanism is commonly employed, it is known to be inadequate⁵. Qualitatively, by considering Jahn-Teller splitting of e_g band of the Mn and invoking strong Hund coupling it is seen that Sr doping corresponds to adding holes in the system. Thus as x increases the resistivity should decrease for low x . Naively one would expect the resistivity to have a minimum at $x = 0.5$; however, the detailed interactions involved in conduction phenomenon could alter this situation. Besides adding holes to the system, Sr doping would also change the lattice parameters due to its different ionic radius as compared to La. The changed overlap integrals would modify the local electronic densities and localization of electrons and holes at different sites in the lattice, thus affecting the transport properties. Coexistence of localized Jahn-Teller polaronic and broad band e_g states may also play important role in these compounds⁶.

X-ray absorption (XA) spectra provide invaluable information about the electronic states of absorbing atom and arrangement of surrounding atoms. An XA edge represents the transition of electron from a core level to the low lying unoccupied states of appropriate symmetry. The edge position of an absorption spectrum depends on electronic charge distribution around the absorbing

atom⁷. A shift in the absorption edge energy is thus a manifestation of the change in the effective charge on the absorbing atom. The effective charge can be varied by changing the number of electrons through appropriate doping and also by changing the interatomic distance. Therefore, in reference to the system under present study, an energy shift in Mn K-edge position on replacing some of trivalent La with divalent Sr will have two contributions: one from the changed number of valence electrons and other from changes in the Mn-O bond length. Further, a change in electronic charge distribution is directly related with localization behaviour of charge carriers and hence electrical transport properties. Therefore, a knowledge of changes in the aforementioned two contributions to the edge shift with Sr concentration will be helpful in understanding the transport properties of manganites. There are many works in the literature reporting XA spectra at Mn K-edge in manganites^{8,9,10,11,12,13}. Almost all this work is concentrated on $\text{La}_{1-x}\text{Ca}_x\text{MnO}_3$ and the change in the edge shift is correlated with the change in the electronic state of Mn ion on Ca doping. Only a few of these studies^{11,12,13} bring out the importance of lattice and band structure effects on the absorption edge, estimation of different contributions to the edge shift and their relation with various physical properties of manganites still remains a challenging task.

In this contribution we show using experimental XA spectra of $\text{La}_{1-x}\text{Sr}_x\text{MnO}_3$ and electronic structure calculations that shift in Mn K-edge position on Sr doping in LaMnO_3 corresponds to the changes in the centre of gravity (CG) of the unoccupied Mn 4*p*-band contributing to the Mn K-edge region. This correspondence is then used to separate the two contributions to the edge shift: one from changed number of valence electrons and the other from changes in Mn-O bond length, which we denote as doping and size contributions, respectively. It is observed that doping contribution to the edge shift with varying Sr concentration follows the observed electrical transport behaviour, which is directly related with localization of

the charge carriers, thus emphasizing the importance of hole localization in governing the transport behaviour of these series of compounds.

II. EXPERIMENTAL AND COMPUTATIONAL DETAILS

Polycrystalline samples of $\text{La}_{1-x}\text{Sr}_x\text{MnO}_3$, $x = 0.0 - 0.7$ were prepared by solid state route. The oxygen content in all the samples was measured by iodometric titration. While the samples with $x = 0.1 - 0.3$ were found to be off-stoichiometric, the samples with $x = 0.4 - 0.7$ were stoichiometric within the experimental accuracy. XA spectra were recorded at room temperature (300 K) on beamline X-18 B using a Si(111) channel cut monochromator at the National Synchrotron Light Source, Brookhaven National Laboratory. The details of sample preparation and experiments are given elsewhere^{14,15}. As shown in our earlier EXAFS work on $\text{La}_{1-x}\text{Sr}_x\text{MnO}_3$ ¹⁵, MnO_6 octahedron is distorted throughout the series and four Mn-O bonds have same bond length and other two have different bond lengths. Therefore, for the purpose of band structure calculations, the local structure was represented by a tetragonal lattice in the whole range, $x = 0$ to 0.7, with interchange of lattice parameters a and c at $x = 0.4$ to account for the change in local structure around $x = 0.4$. Lattice parameters taken for obtaining the muffin-tin radii were two times of these Mn-O bond lengths. Spin polarized electronic structure calculations were carried out using LMTART 6.61¹⁶. For calculating charge density, full-potential LMTO method working in plane wave representation was used. The charge density and effective potential were expanded in spherical harmonics up to $l = 6$ inside the sphere and in a Fourier series in the interstitial region. The exchange correlation functional of the density functional theory was taken after Vosko, Wilk, and Nussair and the generalized-gradient approximation scheme of Perdew *et al.*¹⁷ was also invoked. (6, 6, 6) divisions of the Brillouin zone along three directions for the tetrahedron integration were used to calculate the density of states. Self-consistency was achieved by demanding the convergence of the total energy to be smaller than 10^{-4} Ry/cell.

III. RESULTS AND DISCUSSION

The experimental XA spectra at Mn K-edge (6539 eV) for $\text{La}_{1-x}\text{Sr}_x\text{MnO}_3$, $x = 0 - 0.7$ together with the ones for Mn_2O_3 (Mn^{3+}) and MnO_2 (Mn^{4+}) are shown in figure 1a. The edge-height for all the spectra is normalized to unity. The edge energy E_0 has been taken as the energy position of the first inflection point on the absorption edge. It is evident from the figure that E_0 of all the $\text{La}_{1-x}\text{Sr}_x\text{MnO}_3$ spectra lie between the edge energies for the absorption edge of Mn_2O_3 and MnO_2 with Mn in 3+

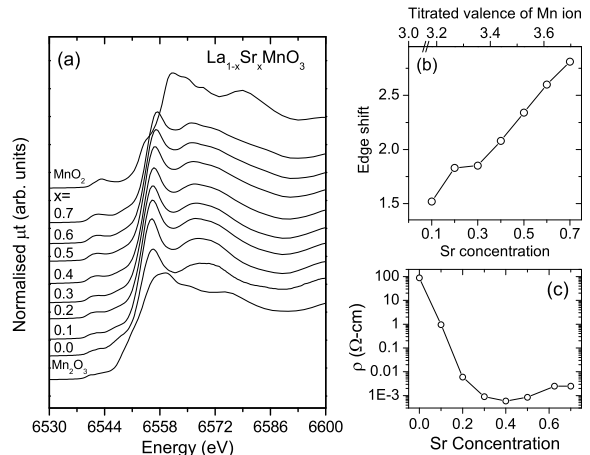


FIG. 1: (a) Experimental Mn K-edge x-ray absorption spectra for Mn_2O_3 , MnO_2 and $\text{La}_{1-x}\text{Sr}_x\text{MnO}_3$, $x = 0 - 0.7$. (b) Edge shift in Mn K-edge with respect to LaMnO_3 and (c) resistivity at 300 K (from [4] and [23]) for $\text{La}_{1-x}\text{Sr}_x\text{MnO}_3$.

and 4+ valence states, respectively. All the absorption spectra also exhibit three pre-edge features; these will be discussed elsewhere.

The edge shift for $\text{La}_{1-x}\text{Sr}_x\text{MnO}_3$, $x = 0 - 0.7$ measured from the absorption edge position of parent compound LaMnO_3 is shown in figure 1b. As seen from the figure this edge shift increases monotonically with increase in Sr concentration and the Mn valence as determined from the iodometric titration. As remarked earlier, these shifts have both doping and size contributions; below we discuss how these two contributions can be separated using band structure calculations. In order to do so, we first establish that the shift in the absorption edge energy on Sr doping can be related with the shift in the CG of the Mn 4p band contributing to the absorption edge. Then we establish that the total shift in CG is sum of shifts in CG due to doping and size contributions explicitly for $x = 0.5$ and 1.0, as they are computationally less demanding. This additive character of doping and size contributions to the edge shift is used to obtain the doping contribution from the experimental edge shift and calculated size contribution for all other compounds of the series. Then we discuss how these contributions are used to understand the transport behaviour of these compounds in a simple manner.

In figure 2, the upper panels show the experimental Mn K-edge absorption spectra for LaMnO_3 , $\text{La}_{0.5}\text{Sr}_{0.5}\text{MnO}_3$ and SrMnO_3 , and the lower two sets of panels show the calculated Mn 4p and O 2p partial density of unoccupied states (PDOS) per formula unit for these compounds. The calculated PDOS agree well with the reported ones by Ravindran *et al.*¹⁸. The PDOS of only p symmetric states is shown since for K-edge only $s \rightarrow p$ transition is dipole allowed and thus is relevant for the present dis-

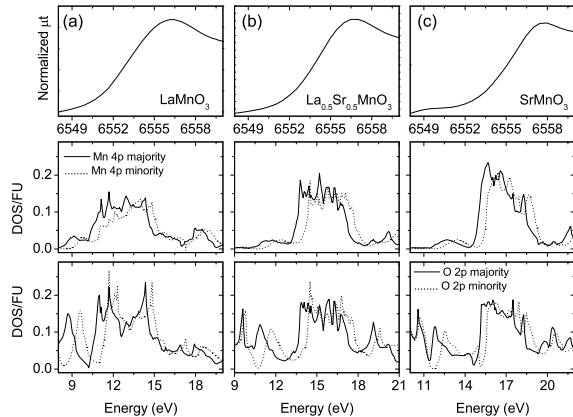


FIG. 2: Experimental Mn K-edge x-ray absorption edge (top panel), calculated spin polarized partial density of states per formula unit for Mn 4p (middle panel) and O 2p (lower panel) of (a) LaMnO₃, (b) La_{0.5}Sr_{0.5}MnO₃ and (c) SrMnO₃.

cussion. The contribution of O 2p unoccupied states is minimal to the absorption edge as it involves a matrix element with wave functions centred on spatially separated atoms; therefore, we discuss only about the CG of Mn 4p band. The edge position corresponds to the difference between 1s and 4p levels; we note that 1s energy with respect to Fermi level hardly changes (~ 0.02 eV) with x , and the edge shift is given by that in 4p band only. The value of average of CG of Mn 4p majority and minority bands for these three compounds is 12.99, 15.65 and 16.94 eV, respectively. Thus the shift in CG for La_{0.5}Sr_{0.5}MnO₃ and SrMnO₃ with respect to LaMnO₃ is 2.66 and 3.95 eV, respectively. Similarly, the Mn K-edge energy for these compounds is 6551.88, 6554.22 and 6555.67 eV with corresponding shifts in E_o for 50% doped and SrMnO₃ compounds being 2.34 and 3.79 eV, respectively. The shift in CG is thus approximately same (within ~ 0.3 eV) as the shift in absorption edge energy. Such behaviour is also seen for shifts in average CG and E_o for CaMnO₃ with respect to LaMnO₃. This indicates that the edge shift can be understood in terms of the shift in the CG of Mn 4p band contributing to the main Mn K-edge and thus CG can be used to monitor the changes in the edge shift. Such an identification of the edge-shift with the shift in CG of the DOS of the contributing band to the absorption edge would be applicable when this DOS has 'one peak' structure. However, when the unoccupied DOS is spread over different 'peaks' in the absorption edge region, corresponding structures will be seen on the edge; a separate inflection point can be identified for each structure which would correspond to the CG of the appropriate energy domain of the band structure. This we have explicitly verified for binary compound MnO whose Mn K-edge is structured. Our calculations also show that the total shift in average CG is less than 0.2 eV when different magnetic ordering

(i.e. FM, C-AFM, A-AFM) are considered. This would indicate that edge shift does not depend much on type of magnetic ordering in conformity with earlier results¹¹. Henceforth, correspondence of E_o with CG obtained from the calculations for the FM phase only is considered.

We now show using the instances of La_{0.5}Sr_{0.5}MnO₃ and SrMnO₃ that the shift in CG can be used to separate out the doping and size contributions to the edge shift. For other values of x , it is rather involved as the necessary unit cell would be too big and contain a much larger number of atoms. The band structure calculations for $x = 0.5$ compound were done using following three lattice models to separate out the doping and size contributions: (a) using Mn-O bond lengths of $x=0.5$ compound obtained from EXAFS thus representing the size contribution with respect to the parent compound LaMnO₃, (b) using the Mn-O bond lengths of LaMnO₃ and replacing 50 % of La atoms by Sr thus representing the doping contribution with respect to LaMnO₃ and (c) using bond lengths corresponding to La_{0.5}Sr_{0.5}MnO₃ and replacing 50% La atoms by Sr by doubling the unit cell, thus considering both doping and size contributions together. The shift in average CG of Mn 4p band with respect to that of LaMnO₃ obtained from (a) and (b) are 1.32 and 1.28 eV, respectively. The summation of these two shifts is 2.60 eV, approximately equal to a shift of 2.66 eV obtained from (c). Similarly, the calculated values of doping and size contributions for SrMnO₃ are 2.35 eV and 1.81 eV, respectively. The summation of these two is 4.16 eV, which is close to the calculated value of 3.95 eV when both doping and size contributions are considered together. Thus the edge shift Δ (and the shift in CG of Mn 4p band) can be written as $\Delta = E_d + E_s$ where E_d and E_s are doping and size contributions to the edge shift, respectively. This indicates that such a strategy could be adopted to determine these two contributions to the edge shift. Therefore, we now calculate E_s for rest of the compounds and estimate E_d by subtracting it from the edge shift observed experimentally.

In figure 3, the shifts in CG with respect to the CG of LaMnO₃ due to size and doping contributions are shown by open and solid circles, respectively, indicating that E_s increases monotonically with Sr concentration whereas E_d first decreases between $x = 0.1 - 0.4$ and then increases as x is increased to 0.7. On extrapolating E_s for $x < 0.1$, E_s approaches zero as x tends to zero. This is shown by plus signs in the figure. The small rate of increase in E_s in this region is consistent with the observed very little change in Mn-O bond lengths between Mn valence of 3.0 and ~ 3.15 ¹⁹. The doping contribution should also vanish at $x = 0$ as the edge shift is measured with respect to LaMnO₃. This would imply that E_d will increase in this region as indicated by the cross signs in the figure.

A look at figure 1c clearly shows that the behaviour of resistivity with x is very similar to the behaviour of E_d for $x \geq 0.1$ - it first decreases with x up to 0.4 and then increases. As discussed above the doping contribution E_d arises due to changes in electronic configuration only

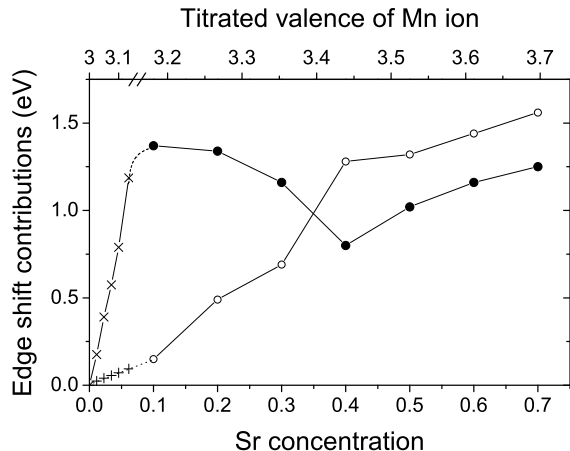


FIG. 3: The doping (close circles) and size (open circles) contributions to the x-ray absorption Mn K-edge shifts for $\text{La}_{1-x}\text{Sr}_x\text{MnO}_3$ with respect to LaMnO_3 . The cross and plus signs correspond to the expected behaviour of doping and size contributions, respectively, when the valence state of Mn ions is $< \sim 3.15$.

keeping the Mn-O bond lengths as in LaMnO_3 . Thus doping contribution is basically representing the effect of hole doping on edge shift. A decrease in E_d between $x = 0.1 - 0.4$ would thus mean that on doping there is a decrease in the number of localized holes. This result is surprising as one would have expected E_d to increase with x as the number of holes increases with increase in Sr doping. It may be remarked here that all the doped holes may not be localized; they may exist simultaneously in localized and delocalized states as suggested by Ramakrishnan *et al.*⁶. We directly correlate E_d with observed resistivity by considering hole localization. The decrease in E_d would mean that holes delocalize between $0.1 \leq x \leq 0.4$. Holes indeed dominate the transport behaviour of manganites in this range of doping as is evident from the Hall effect measurements^{20,21,22}. Since delocalization of holes increases up to $x = 0.4$, such a delocalization should result in decrease in resistivity as

has been observed experimentally²³ (see figure 1c). For $x > 0.4$, the holes start localizing at Mn sites as is evident from the increase in E_d . This would imply that for higher compositions hole localization shall lead to increase in resistivity. This is in conformity with the observed increase in room temperature resistivity⁴.

For $x < 0.1$, E_d should increase with x as shown by the extrapolation, indicating increased hole localization. In the first instance it would mean that resistivity should increase with x as observed for $x > 0.4$. However, experimentally observed behaviour of resistivity is opposite *i.e.* it decreases with x . This behaviour can be understood by noting that the compounds in this region are insulating and the conduction process may be similar to that in semiconductors. Therefore, here the effect of increase in number of holes due to doping may be the dominating phenomenon contributing to the decrease in resistivity.

IV. CONCLUSIONS

In conclusion, we have shown using a simple model based on first principle calculations and experimental x-ray absorption spectra that the energy shift in Mn K-edge on Sr doping in LaMnO_3 has two contributions, namely doping and size contributions. While the doping contribution to Mn K-edge shift arises due to changed number of valence electrons, the changes in Mn-O bond length leads to size contribution. It is observed that the observed doping contribution with varying Sr concentration follows the observed resistivity behaviour. It is discussed that the changes in doping contribution is directly related with the localization of charge carriers thus bringing out the importance of hole localization in understanding the electrical transport properties of these compounds.

Acknowledgments

RB and SKP thank UGC-DAE CSR for financial support. AK thanks CSIR, Government of India for the senior research associate position (pool scheme) during part of this work.

* Present address: Department of Condensed Matter Physics and Material Sciences, Tata Institute of Fundamental Research, Homi Bhabha Road, Kolaba, Mumbai-400 005, India.; Electronic address: sk'iuc@rediffmail.com

† Present address: Material Science Division, Indira Gandhi Center for Atomic Research, Kalpakkam, India.

‡ Present address: Department of Physics, Institute of Science and Laboratory Education, IPS Academy, Indore 452 012, India.

§ Electronic address: avp@csr.ernet.in

¹ M. Imada, A. Fujimori, and Y. Tokura, Rev. Mod. Phys. **70**, 1039 (1998).

² J. M. Coey, M. Virett, and S. V. Molnar, Adv. Phys. **48**, 167 (1999).

³ E. Dagotto, T. Hotta, and A. Moreo, Phys. Rep. **344**, 1 (2001).

⁴ J. Hemberger *et al.*, Phys. Rev. B **66**, 094410 (2002).

⁵ A. J. Millis, Nature **392**, 147 (1998); A. J. Millis *et al.*, Phys. Rev. Lett. **74**, 5144 (1995).

⁶ T. V. Ramakrishnan *et al.*, Phys. Rev. Lett. **92**, 157203 (2004).

⁷ L. V. Azaroff, X-ray spectroscopy (Mc Graw Hill, NY, 1974).

⁸ M. Croft *et al.*, Phys. Rev. B **55**, 8726 (1997).

- ⁹ G. Subias *et al.*, Phys. Rev. B **56**, 8183 (1997).
- ¹⁰ J. Garcia *et al.*, J. Phys.: Condens. Matter **13**, 3229 (2001).
- ¹¹ A. Y. Ignatov *et al.*, Phys. Rev. B **64**, 014413 (2001).
- ¹² F. Bridges *et al.*, Phys. Rev. B **63**, 214405 (2001).
- ¹³ Q. Qian *et al.*, Phys. Rev. B **64**, 024430 (2001).
- ¹⁴ R. Bindu, Eur. Phys. J. B **37**, 321 (2004).
- ¹⁵ R. Bindu *et al.*, J. Phys.: Condens. Matter **17**, 6393 (2005).
- ¹⁶ S. Y. Savrasov, Phys. Rev. B **54**, 16470 (1996).
- ¹⁷ J. P. Perdew, K. Burke, and M. Ernzerhof, Phys. Rev. Lett. **77**, 3865 (1996).
- ¹⁸ P. Ravindran *et al.*, Phys. Rev. B **65**, 064445 (2002).
- ¹⁹ T. Shibata, B. A. Bunker and J. F. Mitchell, Phys. Rev. B **68**, 024103 (2003).
- ²⁰ I. Gordon *et al.*, Phys. Rev. B **62**, 11633 (2000).
- ²¹ P. Majumdar *et al.*, Phys. Rev. B **59**, 4746 (1999).
- ²² A. Asamitsu and Y. Tokura, Phys. Rev. B **58**, 47 (1998).
- ²³ A. Urushibara *et al.*, Phys. Rev. B **51**, 14103 (1995).